



**HAL**  
open science

# Deuterium adsorption on (and desorption from) SiC(0001)-(3x3), $(\sqrt{3} \times \sqrt{3})R30^\circ$ , $(6\sqrt{3} \times 6\sqrt{3})R30^\circ$ and quasi-free standing graphene obtained by hydrogen intercalation

François C. Bocquet, Régis Bisson, Jean-Marc Themlin, J.-M. Layet, Thierry Angot

## ► To cite this version:

François C. Bocquet, Régis Bisson, Jean-Marc Themlin, J.-M. Layet, Thierry Angot. Deuterium adsorption on (and desorption from) SiC(0001)-(3x3),  $(\sqrt{3} \times \sqrt{3})R30^\circ$ ,  $(6\sqrt{3} \times 6\sqrt{3})R30^\circ$  and quasi-free standing graphene obtained by hydrogen intercalation. Journal of Physics D: Applied Physics, 2014, 47 (9), pp.094014. 10.1088/0022-3727/47/9/094014 . hal-00945850

**HAL Id: hal-00945850**

**<https://hal.science/hal-00945850>**

Submitted on 18 Nov 2015

**HAL** is a multi-disciplinary open access archive for the deposit and dissemination of scientific research documents, whether they are published or not. The documents may come from teaching and research institutions in France or abroad, or from public or private research centers.

L'archive ouverte pluridisciplinaire **HAL**, est destinée au dépôt et à la diffusion de documents scientifiques de niveau recherche, publiés ou non, émanant des établissements d'enseignement et de recherche français ou étrangers, des laboratoires publics ou privés.

# Deuterium adsorption on (and desorption from) SiC(0001)- (3×3), ( $\sqrt{3}\times\sqrt{3}$ )R30°, ( $6\sqrt{3}\times6\sqrt{3}$ )R30° and quasi-free-standing graphene obtained by hydrogen intercalation

F C Bocquet<sup>1</sup>, R Bisson<sup>2</sup>, J-M Themlin<sup>3</sup>, J-M Layet<sup>2</sup> and T Angot<sup>2</sup>

<sup>1</sup>Peter Grünberg Institut (PGI-3), Forschungszentrum Jülich - 52425 Jülich, Germany

<sup>2</sup>Aix-Marseille Université, PIIM, CNRS, UMR 7345, 13013 Marseille, France

<sup>3</sup>Aix-Marseille Université, IM2NP, 13397, Marseille, France and CNRS, UMR 7334, 13397, Marseille - Toulon, France

E-mail : regis.bisson@univ-amu.fr

## Abstract.

We present a comparative High-Resolution Electron Energy-Loss Spectroscopy (HREELS) study on the interaction of atomic hydrogen and deuterium with various reconstructions of SiC(0001). We first show that on both the (3×3) and ( $\sqrt{3}\times\sqrt{3}$ )R30° reconstructions, deuterium atoms only bind to silicon atoms, thereby confirming the silicon-rich appellation of these reconstructions. Deuterium passivation of the (3×3) is only reversible when exposed to atomic deuterium at a surface temperature of 700 K since tri- and dideuterides, necessary precursors for silicon etching, are not stable. On the other hand, we show that the deuteration of the ( $\sqrt{3}\times\sqrt{3}$ )R30° is always reversible because precursors to silicon etching are scarce on the surface. Then, we demonstrate that hydrogen (deuterium) adsorption at 300 K on both the ( $6\sqrt{3}\times6\sqrt{3}$ )R30° (buffer-layer) and the quasi-free-standing graphene occurs on carbon atoms justifying their carbon-rich appellation. Comparison of the deuterium binding in the intercalation layer of quasi-free-standing graphene with the deuterated ( $\sqrt{3}\times\sqrt{3}$ )R30° surface provides some indication on the bonding structure at the substrate intercalation layer. Finally, by measuring C-H (C-D) vibrational frequencies and hydrogen (deuterium) desorption temperatures we suggest that partial sp<sup>2</sup>-to-sp<sup>3</sup> rehybridization occurs for the carbon atoms of the buffer-layer because of the corrugation related to covalent bonding to the SiC substrate. In contrast, on quasi-free-standing graphene hydrogen (deuterium) atoms adsorb very similarly to what is observed on graphite, i.e. without preferential sticking related to the underlying SiC substrate.

(Some figures in this article are in color only in the electronic version)

PACS numbers: 81.05.ue, 68.43.Pq, 79.20.Uv, 68.43.-h, 67.63.Gh, 68.47.Fg

## 1. Introduction

Graphene, a single layer of carbon atoms arranged in a honeycomb lattice presents outstanding electronic and mechanical properties. Since its isolation in 2004, it has been widely studied both for a fundamental understanding of its properties as well as for its potential for applications [1]. It was later shown that  $\mu\text{m}$ -large graphene layer could be epitaxially grown on a wide band-gap semiconductor, namely SiC(0001) [2]. However, such a graphene is doped and interacts with the underlying substrate [3]. Hydrogen intercalation can dramatically reduce such an interaction [4] and improve device performances [5,6]. Furthermore, graphene could be more easily integrated into devices if one could chemically (and reversibly) tailor its electronic properties, e.g. by modifying its band-gap [7]. One possibility is to expose the graphene layer to atomic hydrogen, a procedure known to open a wide band gap for graphene supported on metallic substrates [8,9] and which seems to occur also for quasi-free-standing graphene grown on SiC(0001) [10]. Hydrogen adsorption being central to the production and/or modification of quasi-free-standing graphene supported on silicon carbide, it is necessary to gain a detailed understanding of how hydrogen atoms bind to the material at the various stages of production of graphene on SiC(0001).

The creation of quasi-free-standing monolayer graphene (QFMLG) on the SiC semiconductor substrate and the modification of its electronic properties are possible in vacuum through successive steps of thermal annealing and hydrogenation of a commercial sample. Starting from a SiC(0001) wafer, one first anneals the sample under a silicon flux to obtain the silicon-rich  $(3\times 3)$  reconstruction. Further thermal annealing leads to the less silicon-rich  $(\sqrt{3}\times\sqrt{3})R30^\circ$  reconstruction. By reaching an annealing temperature of 1450 K, the surface silicon atoms sublimation is complete and the carbon-rich  $(6\sqrt{3}\times 6\sqrt{3})R30^\circ$  reconstruction of SiC(0001) is obtained. The latter reconstruction, often called the buffer-layer, consists of a graphene-like layer which remains covalently bound to the SiC substrate [11]. A well decoupled quasi-free-standing monolayer graphene (QFMLG) is obtained from the buffer-layer by hydrogenation of the  $(6\sqrt{3}\times 6\sqrt{3})R30^\circ$  sample maintained at a temperature of 950 K [10,12]. Finally, a drastic reduction of the density of electronic states near the Fermi level, probably related to a band gap opening, results from the adsorption of hydrogen atoms on QFMLG at room temperature. The quasi-free-standing monolayer graphene can be recovered by annealing the hydrogenated sample above 600 K [10].

In this article we characterize the surface structure and silicon/carbon atoms coordination of all these SiC(0001) reconstructions using hydrogen (deuterium) adsorption/desorption probed by vibrational spectroscopy and Low-Energy Electron Diffraction (LEED). These techniques and other experimental details are the subject of Section 2. Results obtained on the  $(3\times 3)$  and the  $(\sqrt{3}\times\sqrt{3})R30^\circ$  silicon-rich reconstructions of SiC(0001) are presented in Section 3, while Section 4 is dedicated to the carbon-rich  $(6\sqrt{3}\times 6\sqrt{3})R30^\circ$  reconstruction and QFMLG. Section 5 concludes this article.

## 2. Experimental methods

All samples were prepared and measured in an Ultra-High Vacuum (UHV) apparatus equipped with a VSI Delta 0.5 High-Resolution Electron Energy-Loss Spectrometer (HREELS), an Omicron 4-grid LEED and a source of atomic hydrogen of the hot capillary type (Omicron EFM-H). We used a semi-insulating 6H-SiC(0001) wafer (carrier concentration  $\sim 10^{15} \text{ cm}^{-3}$ , supplied by TankeBlue), to make  $\sim 1 \text{ cm}^2$  samples. Thermal annealing was performed by radiative heating from a tungsten filament for temperatures below 1300 K and by an additional electronic bombardment on the backside of the sample for temperatures above 1300 K. A K-type thermocouple attached in the vicinity of the SiC(0001) sample was used to determine its temperature with a  $\pm 5\%$  reproducibility. It was calibrated against a dummy sample on which another thermocouple was glued.

Preparation and cleaning of various SiC reconstructions can be obtained with high and/or low pressure methods. High pressure methods (e.g. [13]) such as annealing in  $\text{H}_2$  and/or Ar atmosphere generally give atomically flat and large terraces [14] but cannot lead to the  $(3 \times 3)$  reconstruction. On the other hand, low pressure methods give access to a larger set of reconstructions with the possibility to reversibly retrieve reconstructions by using silicon atoms flux. In this study, we directly introduced in the UHV preparation chamber (base pressure  $< 2.10^{-10} \text{ mbar}$ ) the SiC(0001) sample which is first outgassed by repeated annealing cycles below 1100 K. We prepare the  $(3 \times 3)$  reconstruction by annealing the sample at 1150 K while being exposed to a flux of silicon atoms generated by a Si wafer resistively heated at  $\sim 1450 \text{ K}$ . Heating the  $(3 \times 3)$  surface at 1300 K leads to the formation of the  $(\sqrt{3} \times \sqrt{3})R30^\circ$  reconstruction. Further annealing at 1450 K creates the  $(6\sqrt{3} \times 6\sqrt{3})R30^\circ$  buffer-layer. Quasi-free-standing monolayer graphene is finally obtained by heating the buffer-layer at 950 K while exposing to a fluence of  $\sim 5.10^{17} \text{ cm}^{-2}$  hydrogen atoms. The preparation quality of the  $(3 \times 3)$ ,  $(\sqrt{3} \times \sqrt{3})R30^\circ$ ,  $(6\sqrt{3} \times 6\sqrt{3})R30^\circ$  and QFMLG samples was assessed by checking their LEED patterns for different electron incident energies as well as their HREEL spectra (see [10] and supplemental materials therein). All measurements were obtained at room temperature. For structural characterization purpose, all reconstructions were exposed to hydrogen (deuterium) with atomic flux in the  $10^{14}$ - $10^{15} \text{ atoms.cm}^{-2}.\text{s}^{-1}$  range. For silicon-rich reconstructions,  $(3 \times 3)$  and  $(\sqrt{3} \times \sqrt{3})R30^\circ$ , deuterium exposure was first performed at 700 K to avoid silicon atoms etching which is known to occur below 600 K for Si(100) and Si(111) [15,16]. Then all SiC reconstructions were exposed to hydrogen (deuterium) atoms at room temperature. Note that the  $(3 \times 3)$  and  $(\sqrt{3} \times \sqrt{3})R30^\circ$  reconstructions have not been exposed to hydrogen because the characteristic vibrational scissor/umbrella modes of  $\text{SiH}_2$  and  $\text{SiH}_3$  hydrides are expected at a similar loss energy than the intense SiC Fuchs-Kliwer phonons.

Hydrogen (deuterium) desorption from the different SiC(0001) surfaces were studied by gradually increasing the temperature of the sample in several temperature steps of typically 50 – 100 K. Between each temperature step, the sample was cooled to 300 K and then characterized by LEED and HREELS. For the  $(6\sqrt{3}\times 6\sqrt{3})R30^\circ$  and QFMLG samples, the Full-Width at Half-Maximum (FWHM) of the elastic peak of the HREEL spectra was used to evaluate the presence of hydrogen on the surface. As shown in section 4.1 and section 4.2, hydrogen adsorption on these two carbon-rich surfaces leads to a dramatic diminution of the HREELS elastic peak FWHM and therefore serves as a fast and precise indicator of the presence/absence of hydrogen on the surface.

### 3. Silicon-rich reconstructions of SiC(0001)

#### 3.1. The $(3\times 3)$ reconstruction

Starke and coworkers have shown with LEED, STM and DFT calculations [17,18] that the SiC(0001)- $(3\times 3)$  reconstruction is a silicon-rich surface consisting of a silicon adlayer terminated by tetrahedral clusters of silicon (Figure 1a). These clusters are composed of four silicon atoms and possess only one dangling bond located on the topmost atom. Therefore it can accommodate only one hydrogen atom if its integrity has to be conserved. Hydrogen (deuterium) adsorption on this surface has been studied experimentally with HREELS [19,20] and Temperature Programmed Desorption (TPD) [21], confirming that silicon atoms are terminating the  $(3\times 3)$  reconstruction. However, upon hydrogenation, the LEED pattern changes to a  $(1\times 1)$  structure, raising questions regarding the stability of silicon clusters and its recovery upon hydrogen desorption. Hydrogen desorption from this  $(1\times 1)$  surface has led to less consensus since some groups have found that the  $(3\times 3)$  reconstruction can be retrieved upon annealing [22,23] while other groups have not [20,24]. Proponents of the hydrogenation irreversibility of the  $(3\times 3)$  surface proposed that silicon atoms are etched upon hydrogenation i.e. silicon atoms bonds in the cluster are broken in order to accommodate further hydrogen atoms until Si-H<sub>4</sub> gaseous molecules are formed, which would explain the observed influence of the hydrogen atom dose onto the reversibility of the hydrogenation [20]. From one study to the other the actual doses used to hydrogenate samples are plagued with large uncertainties because tungsten filaments were used to dissociate H<sub>2</sub> and their distance to the sample varies, which could also change the sample temperature during hydrogenation because of the filament induced radiative heating. We revisited the reversibility of the hydrogenation of the SiC(0001)- $(3\times 3)$  surface using a thermally shielded and dose-calibrated atomic source.

Figure 2 compares the HREEL spectra of the  $(3\times 3)$  surface after exposure to  $\sim 10^{17}$  atoms.cm<sup>-2</sup> of deuterium atoms at 700 K and after exposure to  $\sim 10^{17}$  atoms.cm<sup>-2</sup> of deuterium atoms at 300 K. Table 1 summarizes the spectroscopic signatures we measured for these preparations (as well as for all

samples presented in this article) and literature values for silicon and carbonaceous surfaces. In HREEL spectra of every SiC(0001) reconstruction and QFMLG in this article, the most intense vibrational peaks located around 115 – 117 meV and its multiples are related to the well-known Fuchs-Kliwer phonons (FK) [25]. The small shifts of this peak from one reconstruction to another were already reported elsewhere [26] and will not be discussed in this article.

Deuterium adsorption on the silicon terminated (3×3) surface is evidenced in HREELS by the appearance of the Si-D<sub>x</sub> stretch vibration at 189 meV both for the 700 K and 300 K deuterium exposure. The vibrational mode at 81 meV is only measured when the deuterium dose has been performed at 300 K and can correspond to both the SiD<sub>2</sub> scissor mode and the SiD<sub>3</sub> umbrella mode given the resolution and the irregular background of spectra. The absence of the SiD<sub>2</sub>/SiD<sub>3</sub> modes for deuterium exposure at 700 K is consistent with observations on silicon surfaces where the maximum desorption rate for SiD<sub>2</sub>/SiD<sub>3</sub> species is found below 700 K [15,16]. Note that C-D vibrations are not observed consistently with the silicon-rich nature of the (3×3) surface.

Figure 3 shows the LEED pictures of the (3×3) surface after preparation, after exposure to ~ 10<sup>17</sup> atoms.cm<sup>-2</sup> of deuterium atoms and after deuterium desorption following a thermal annealing at 850 K. While deuterium adsorption at 300 K or 700 K both leads to a (1×1) structure (Figure 3b), deuterium desorption leads to markedly different LEED patterns for samples deuterated at 300 K or 700 K. Only the surface deuterated at 700 K fully recovers the intact (3×3) structure upon thermal annealing (Figure 3c) whereas the 300 K deuterated sample develops a LEED pattern presenting additional diffraction spots to the (3×3) structure (indicated by arrows in Figure 3d). This demonstrates that deuteration of SiC(0001)-(3×3) is reversible only when deuteration is performed at 700 K, i.e. when Si-D<sub>2</sub>/Si-D<sub>3</sub> species are absent on the surface. This observation can be rationalized from the work of Dinger *et al.* on the etching of hydrogenated (deuterated) Si(100) and Si(111) [15,16]. In these studies, it was shown that the generation of gaseous silane from etching of silicon surface atoms happens during thermal annealing only when the surface is dosed with atomic hydrogen at temperature below 700K, the temperature below which adsorbed etching precursors (SiH<sub>2</sub> and SiH<sub>3</sub>) are present at the surface. Similarly, our HREELS data shows that precursors to silicon etching are stable on SiC(0001)-(3×3) at 300 K but not at 700 K. Therefore deuterium desorption prevents to recover the (3×3) reconstruction for sample exposed to deuterium at 300 K because of etching. In contrast, for sample exposed to deuterium at 700 K, the (3×3) reconstruction can be retrieved upon desorption.

### 3.2. The (√3×√3)R30° reconstruction

It has been shown experimentally with LEED and photoelectron spectroscopy [19,27], that the SiC(0001)-(√3×√3)R30° reconstruction is a silicon-rich surface consisting of silicon adatoms located

on the  $T_4$  fourfold top positions above three silicon atoms (Figure 1b) and possessing a single dangling bond, consistent with previous theoretical calculations [28]. Hence, the accommodation of more than one hydrogen atom is possible only at the expense of the adatoms back bonds. Hydrogen adsorption on the  $(\sqrt{3}\times\sqrt{3})R30^\circ$  surface has been studied experimentally with HREELS and TPD, confirming that the surface termination species is silicon. Like for the  $(3\times 3)$  surface, the LEED pattern changes to  $(1\times 1)$  upon hydrogenation pointing to surface structural change. It is therefore natural to wonder whether hydrogen desorption leads to any alteration of the  $(\sqrt{3}\times\sqrt{3})R30^\circ$  reconstruction.

Figure 4 shows the HREEL spectra obtained for the  $(\sqrt{3}\times\sqrt{3})R30^\circ$  after exposure to  $\sim 10^{17}$  atoms.cm<sup>-2</sup> of deuterium atoms at 700 K and after exposure to  $\sim 10^{17}$  atoms.cm<sup>-2</sup> of deuterium atoms at 300 K and measured vibrational frequencies are presented in Table 1. Adsorption of deuterium on the silicon atoms of the surface is evidenced by the occurrence of SiD<sub>x</sub> stretch vibration at 192 meV for exposure at 700 K and 300 K. The stretch vibration on the  $(\sqrt{3}\times\sqrt{3})R30^\circ$  surface is 3 meV higher in energy than on the  $(3\times 3)$  surface. We attribute this small shift, already observed with hydrogen by Tautz *et al.* [19], to the different chemical environments of deuterides rather than a preferential occurrence of dideuterides over monodeuterides since this shift is present even in the absence of dideuterides for a deuterium exposure at 700K. Another difference between the  $(3\times 3)$  and  $(\sqrt{3}\times\sqrt{3})R30^\circ$  surfaces is the presence of a clear and sharp Si-D bending mode at 67 meV only visible on the  $(\sqrt{3}\times\sqrt{3})R30^\circ$  reconstruction. On the  $(3\times 3)$  reconstruction a succession of less peaked features are present in this range of frequency, similar to the case of pure silicon surfaces where deuterium bending modes and phonons of the silicon surfaces are mixing [29]. Finally, on the  $(\sqrt{3}\times\sqrt{3})R30^\circ$  surface Si-D<sub>2</sub>/Si-D<sub>3</sub> vibrational signatures at 81 meV are present only for 300 K deuterium exposure, like on the  $(3\times 3)$  surface. However, the relative strength of the stretch vibration to the Si-D<sub>2</sub>/Si-D<sub>3</sub> vibration is almost inverted on the  $(\sqrt{3}\times\sqrt{3})R30^\circ$  as compared to the  $(3\times 3)$  surface. Note that on the  $(3\times 3)$  surface exposed at 300 K, the stretch vibration is broadened and increased in intensity because of a superposition with the FK+Si-D<sub>2</sub>/Si-D<sub>3</sub> multiple loss. In the case of the  $(\sqrt{3}\times\sqrt{3})R30^\circ$ , the Si-D<sub>2</sub>/Si-D<sub>3</sub> signature is barely visible while the stretch vibration is intense, suggesting that Si-D monodeuteride species are outnumbering rare Si-D<sub>2</sub>/Si-D<sub>3</sub> species.

Figure 5 shows the LEED spectra of the  $(\sqrt{3}\times\sqrt{3})R30^\circ$  surface after preparation, after exposure to  $\sim 10^{17}$  atoms.cm<sup>-2</sup> of deuterium atoms at 300 K and 700 K, and after deuterium desorption following thermal annealing at 1050 K. Deuterium adsorption at 300 K or 700 K both leads to a  $(1\times 1)$  structure and thermal annealing of both preparations allows the recovery of the  $(\sqrt{3}\times\sqrt{3})R30^\circ$  LEED pattern. Note that a thermal annealing at 910 K is not sufficient to fully recover the  $(\sqrt{3}\times\sqrt{3})R30^\circ$  LEED pattern, consistently with hydrogenated SiC(0001)- $(1\times 1)$  samples obtained with high pressure methods [13], i.e. deuterium atoms need a higher temperature to desorb from the  $(\sqrt{3}\times\sqrt{3})R30^\circ$  than from the  $(3\times 3)$  SiC reconstruction and pure silicon surfaces. This indicates that deuterium on the  $(\sqrt{3}\times\sqrt{3})R30^\circ$

reconstruction is more strongly bound to the silicon atoms consistently with the higher stretching frequency on  $(\sqrt{3}\times\sqrt{3})R30^\circ$  than on  $(3\times 3)$ .

The reversibility of the  $(\sqrt{3}\times\sqrt{3})R30^\circ$  surface toward deuterium adsorption/desorption observed by LEED has also been reported by other groups with hydrogen [21,30], confirming that silicon etching is negligible on the hydrogenated/deuterated  $(\sqrt{3}\times\sqrt{3})R30^\circ$ . Silicon etching during thermal annealing necessitates neighboring Si-D<sub>2</sub> (Si-H<sub>2</sub>) and Si-D<sub>3</sub> (Si-H<sub>3</sub>) species in order to form gaseous silane molecules [15]. Our HREELS data suggest that Si-D<sub>2</sub>/Si-D<sub>3</sub> etching precursors are minority species. Hence, the observed negligible silicon loss on this silicon-rich surface can be rationalized either by a too low density of neighboring Si-D<sub>2</sub> and Si-D<sub>3</sub> deuterides or by the absence of one of those two deuterides. TPD spectra from Aoki and Hirayama show only two peaks for hydrogen desorption from  $(\sqrt{3}\times\sqrt{3})R30^\circ$  [21], in contrast to the three peaks observed on  $(3\times 3)$  and on Si(100) which are attributed, in the increasing order of desorption temperature, to the desorption from SiH<sub>3</sub>, SiH<sub>2</sub> and SiH species. The two desorption temperatures observed by TPD on the  $(\sqrt{3}\times\sqrt{3})R30^\circ$  surface suggest that solely Si-H<sub>3</sub> and Si-H species are present on this surface. Based on ion scattering techniques, Fujino *et al.* [30] have also proposed a model containing only Si-H<sub>3</sub> and Si-H species on the hydrogenated  $(\sqrt{3}\times\sqrt{3})R30^\circ$ . In order to confirm that the hydrogen desorption reversibility of the  $(\sqrt{3}\times\sqrt{3})R30^\circ$  surface is due to the absence of stable Si-D<sub>2</sub> species, vibrational spectra with better resolution would be needed in order to resolve Si-D<sub>2</sub> and Si-D<sub>3</sub> vibrations. Unfortunately, this is a challenging measurement that HREELS or infrared absorption spectroscopy have failed to realize for deuterated silicon so far [29,31]. Finally, we note that Fujino's reconstruction model is consistent with our 300K exposure data, but cannot account for the missing Si-D<sub>2</sub>/Si-D<sub>3</sub> feature of the 700K exposure. Our experimental observation of a  $(1\times 1)$  reconstruction for a solely mono-deuterated  $(\sqrt{3}\times\sqrt{3})R30^\circ$  surface calls for the development of another reconstruction model specific to the mono-hydrogenated reconstruction.

#### 4. Carbon-rich reconstructions of SiC(0001)

##### 4.1. The $(6\sqrt{3}\times 6\sqrt{3})R30^\circ$ reconstruction or so-called "buffer-layer"

The buffer-layer, zeroth-layer or  $(6\sqrt{3}\times 6\sqrt{3})R30^\circ$ , is known to be a carbon-rich reconstruction of SiC(0001) obtained after annealing the silicon-rich  $(\sqrt{3}\times\sqrt{3})R30^\circ$  reconstruction to  $\sim 1450$  K [32]. Further annealing transforms the buffer-layer into a graphene layer with a new buffer-layer formed underneath. Although a matter of debate in recent years [33], the consensus for experimental studies [4,10–12,14,34] as well as for theoretical studies [35–38] is that the buffer-layer consists of a graphene honeycomb structure covalently bound to some of the silicon atoms of the SiC substrate (Figure 1c). This model is supported by the following observations: the topological similarity in STM between the

QFMLG and the buffer-layer with the absence of obvious defects in the formed QFMLG [11], the complete reversibility of the buffer-layer transformation into quasi-free-standing monolayer graphene (QFMLG) with hydrogen intercalation [4,10], and the appearance of Si-H oscillators below the QFMLG [10,34]. Because of this covalent back-bonding and the presence of remaining silicon dangling bonds at the interface (Figure 1c), the carbon honeycomb structures of the buffer-layer is a semi-conducting surface with faint surface states lying in the 0.1 - 0.5 eV range and around 0.9 eV below  $E_F$  [12,39,40]. Hydrogen adsorption on the buffer-layer has only been studied so far with STM apparatuses. Using Scanning Tunneling Spectroscopy (STS), Guisinger *et al.* have shown that the buffer-layer loses its surface states when exposed to atomic hydrogen [41]. Based on the temperature at which these hydrogen desorb ( $\sim 670$  K), Guisinger *et al.* proposed that hydrogen adsorbs on silicon dangling bonds underneath the buffer-layer, even though intercalation-induced quasi-free-standing graphene was not observed. The latter interpretation seems at odds with the recent consensus that the buffer-layer transformation into QFMLG and the concomitant disappearance of surface states occur only for hydrogenation performed around 950 K and needs further investigation.

A characteristic HREEL spectrum of the buffer-layer, measured in specular geometry, is shown in Figure 6. It presents a large elastic peak (Full-Width at Half-Maximum FWHM = 13 meV) and the well-known Fuchs-Kliwer (FK) bulk phonons of SiC, already mentioned in section 3. When exposing this carbon-rich reconstruction to atomic hydrogen at a surface temperature of 300 K, the FWHM decreases to 4.5 meV (Figure 6), a value close to the set resolution of the spectrometer. HREEL spectra recorded in specular geometry are known to be often well described by the dielectric theory [42]. In particular, the shape and width of the elastic peak is related to the density of electronic states near the surface around the Fermi level. Therefore, we attribute the observed reduction of the HREELS elastic peak FWHM upon hydrogenation to the disappearance of the buffer-layer surface states, consistently with previous STS measurements [41].

Figure 7 presents HREEL spectra, recorded in out-of-specular geometry in order to reduce the low energy electronic excitation induced background, for both hydrogenated and deuterated surfaces. Upon isotope substitution, the electron energy losses related to phonon modes of the SiC substrate remain identical while those characteristic of hydrogen (deuterium) adsorption sites are shifted in frequency by a constant factor quantitatively determined by the change of oscillator partner masses (X-H vs X-D). The measured oscillator frequencies related to both hydrogen isotopes adsorbed on the buffer-layer are presented in Table 1. It reveals that hydrogen only adsorbs on carbon atoms of the  $(6\sqrt{3}\times 6\sqrt{3})R30^\circ$ , in agreement with the actual consensus that the buffer-layer fully covers the SiC substrate and that hydrogenation at a sample temperature of 300 K is unable to create QFMLG by intercalation. The absence of any Si-H (Si-D) vibrations signature, contrary to what Guisinger *et al.* proposed [41], implies that the disappearance of the buffer-layer surface states is not due to the direct

adsorption of hydrogen (deuterium) on the silicon dangling bonds. As an alternative explanation, we propose that the hydrogenated buffer-layer carbon atoms induce on their bare neighbor carbon atoms a local  $sp^2$ -to- $sp^3$  rehybridization with an underlying silicon atom bearing a dangling bond and thus making the surface states disappear. A similar  $sp^2$ -to- $sp^3$  rehybridization of neighboring carbon atoms has already been observed for hydrogenated graphene on Iridium [8,43]. This local reconstruction was termed “graphane-like” as one carbon atom binds to a hydrogen and a neighboring carbon atom binds to a substrate surface atom. The similar scenario we propose implies that the buffer-layer is drastically modified upon hydrogenation, which is evidenced by the transformation of the  $(6\sqrt{3}\times 6\sqrt{3})R30^\circ$  LEED pattern of the buffer-layer into a quasi- $(1\times 1)$  pattern (Figure 8). Analysis of our measured hydrogen (deuterium) vibrational frequencies and desorption temperatures further support our interpretation and is discussed below.

As shown in Table 1, stretching frequencies of hydrogen isotopes adsorbed on the buffer-layer are higher from those measured on graphite (and QFMLG, see section 4.2) but similar to the one measured on ion-damaged graphite [44,45] and diamond surfaces [46–49]. Furthermore, Figure 9 shows that hydrogen adsorbed on the buffer-layer desorbs at 750 K, a higher temperature than on graphite but similar to the desorption temperature on ion-damaged graphite [44]. Diamond surfaces and ion-damaged graphite bind more strongly hydrogen atoms, as evidenced by their higher vibrational frequency and higher desorption temperature [44] as compared to graphite. This fact is related to the  $sp^3$  hybridization of the carbon atoms involved in the bonding to hydrogen. Therefore, the measured frequencies and the desorption temperature presented here for hydrogen atoms adsorbed on the buffer-layer show that the carbon atoms involved in hydrogen bonding have a stronger  $sp^3$  character than the carbon atoms on hydrogenated graphite and QFMLG (see section 4.2). This result is consistent with recent Density Functional Theory -based calculations [50] and x-ray photoelectron diffraction measurements [51] which show that the carbon atoms in the bare buffer-layer are already partially  $sp^3$  hybridized, not only the carbon atoms covalently bound to the SiC substrate, but also the other carbon atoms in the honeycomb structure of the buffer-layer. We also note that the spectral width of the hydrogen-related vibrational modes is significantly larger than the elastic peak and the FK features. This can be explained if the hydrogen atoms are bound to a set of carbon atoms with slightly different environment which can originate both from the native long-range corrugation of the bare buffer-layer [51] and the hydrogenation-induced quasi- $(1\times 1)$  reconstruction of the buffer-layer with hybridization to the SiC substrate, as mentioned above. The large spectral width of hydrogen (deuterium) vibrations on the buffer-layer suggests that adsorbed hydrogen atoms experience a large range of binding energy, which seems also corroborated by the larger range of temperature on which hydrogen desorption occurs on the buffer-layer as compared to the case of quasi-free-standing graphene (Figure 9). Our suggestion that the hydrogen binding energy on the buffer-layer presents some

heterogeneity waits for confirmation from other experimental observations, e.g. TPD combined with scanning probe microscopy [52], or theoretical calculations.

#### 4.2. The quasi-free-standing monolayer graphene obtained by hydrogen intercalation

In 2009, Riedl *et al.* showed that it is possible to reversibly transform the buffer-layer and the monolayer graphene into a quasi-free-standing monolayer graphene and quasi-free-standing bilayer graphene, respectively, by intercalating hydrogen atoms underneath the surface plane using sample heating at 900 K in an atmosphere of molecular hydrogen [4]. Later, it was shown that this intercalation technique is feasible in ultra-high vacuum for obtaining both monolayer [10] and bilayer [53] quasi-free-standing graphene using a hydrogen atoms source. Such procedures convert the buffer-layer into quasi-free-standing monolayer graphene (QFMLG) by breaking the bonds between the buffer-layer and the SiC substrate and by passivating the silicon dangling bonds of the SiC substrate with hydrogen atoms [10,34] (Figure 1d). Figure 10a presents a typical HREEL spectrum for a QFMLG sample, measured in specular geometry with an incident energy of 5eV. The important feature of this spectrum is the very large elastic peak (FWHM = 30 meV) which almost completely screens the FK phonon of the SiC substrate and impedes the detection of any other vibrational features. We note that infrared absorption spectroscopy in the attenuated total reflection mode (FTIR-ATR) is able to detect Si-H vibrations from the intercalation at the SiC interface for a similar sample [34], while HREELS is not. A notable difference between HREELS and FTIR-ATR methods is that in the latter case the quasi-free-standing graphene could be perturbed by the contact made between the sample and a germanium prism, and allows the infrared light to couple with the H-Si underneath. A detailed study would be needed to rationalize the differences observed between these two techniques, but it is out of the scope of this article. Figure 10b shows a HREEL spectrum obtained in a loss region up to 10 eV (incident energy 26 eV, specular geometry) for the QFMLG sample. One clearly sees a broad loss feature at about 5.8 eV, absent for the buffer-layer, which we attribute to the  $\pi$ -plasmon of QFMLG, similarly to previous observations for graphene grown atop the buffer-layer [54–56]

After exposing the QFMLG sample to  $3 \times 10^{15}$  atoms.cm<sup>-2</sup> of atomic hydrogen at a surface temperature of 300 K, we observe the FWHM of the HREEL elastic peak to sharply decrease from 30 meV to 4.5 meV (Figure 10a), while the  $\pi$ -plasmon feature vanishes almost completely (Figure 10b). Balog *et al.* [8] and Haberer *et al.* [9] have shown that a gap is opened in the  $\pi$ -band of graphene supported on metals when hydrogen atoms are adsorbed. The hydrogen-induced loss of density of electronic states near the Fermi level in our QFMLG sample, evidenced by the drop of HREELS FWHM as well as the disappearance of the  $\pi$ -plasmon, strongly suggests that a band gap also opens in the  $\pi$ -band of quasi-free-standing graphene supported on SiC(0001). The fact that the LEED spots characteristic of the graphene layer remains similar upon hydrogenation shows that the honeycomb

structure is preserved (Figure 8), consistently with previous measurements on hydrogenated free-standing graphene membrane [57].

The modification of the electronic properties for hydrogenated QFMLG samples reduces the overall background and allows the detection of vibrational modes thus providing chemical information on the bonding configuration of hydrogen at both the graphene surface and at the graphene-SiC interface. In order to discriminate hydrogen bonding related to the intercalation step from hydrogen adsorbed on the quasi-free-standing graphene, we used different hydrogen isotopes for the two preparation steps [10]. The four possible isotope combinations have been realized and on Figure 11 we show the resulting HREEL spectra for the two following combinations: H-QFMLG/D-SiC and D-QFMLG/H-SiC i.e. hydrogenated quasi-free-standing graphene with deuterium intercalation and deuterated quasi-free-standing graphene with hydrogen intercalation, respectively. Besides the LO phonon of graphene [58,59] measured around 193 meV and the FK SiC phonon loss at 115 meV and its multiples, bending and stretching modes of hydrogen (deuterium) adsorbed on carbon and silicon atoms are detected (Table 1). More specifically, only C-D and Si-H modes are detected for the D-QFMLG/H-SiC sample, while only C-H and Si-D modes are detected for the H-QFMLG/D-SiC sample. These observations indicate on one hand that the intercalated hydrogen used to transform the buffer-layer into a QFMLG bind solely to the silicon atoms of the SiC substrate, consistent with the accepted model that the buffer-layer consists in a graphene layer covalently bound to the silicon atoms of the SiC substrate. On the other hand, QFMLG exposed to hydrogen at a surface temperature of 300 K exhibits only hydrogen adsorbed on the carbon atoms of the graphene plane which shows that QFMLG is impermeable to hydrogen atoms at room temperature. Further proof that hydrogenated QFMLG consists in hydrogen atoms adsorbed on the carbon honeycomb structure comes from studying in details their vibrational frequencies and their thermal stability [10].

In contrast to vibrational frequencies of hydrogen and deuterium adsorbed on the buffer-layer (section 4.1), vibrational frequencies of hydrogen isotopes on QFMLG are similar to those measured on graphite (Table 1). Stretching frequencies for C-H and C-D at 331 meV and 243 meV as well as the C-H bending frequency at 152 meV are almost identical to the graphite ones [45], even though some expected vibrational modes are hidden on QFMLG because of the intense FK SiC phonons. Furthermore, using the HREELS technique, we observed a complete desorption of hydrogen adsorbed on QFMLG above 600 K, as shown in Figure 9. Complete desorption of hydrogen on graphite above 600 K has also been reported by Hornekaer *et al.* [52]. Therefore, based on the similarity of vibrational spectra and the desorption temperature, we propose that hydrogen adsorption on QFMLG occurs in dimers and clusters structure as in the case of graphite i.e. without preferential sticking dictated by the underlying SiC substrate. This hydrogen adsorption behavior of the graphene plane is a further indication that QFMLG obtained by hydrogen intercalation is well decoupled from the SiC substrate.

Finally, we consider the hydrogen (deuterium) atoms in the intercalation layer of the QFMLG sample. Figure 9 shows that the intercalated hydrogen/deuterium desorbs above 1100 K, higher than the desorption temperature observed on pure silicon surfaces but close to the value observed for the silicon-rich  $(\sqrt{3}\times\sqrt{3})R30^\circ$  SiC(0001) reconstruction (see section 3.2). Other striking similarities are the presence of a Si-D bending mode at 67 meV in both the intercalation layer of QFMLG and the deuterated  $(\sqrt{3}\times\sqrt{3})R30^\circ$  surface as well as identical stretching frequencies. These analogous vibrational signatures and desorption temperature indicate that the silicon atoms on which intercalated deuterium binds below the QFMLG have a similar environment than the silicon atoms of the deuterated  $(\sqrt{3}\times\sqrt{3})R30^\circ$ . Therefore, we propose that the  $(6\sqrt{3}\times6\sqrt{3})R30^\circ$  buffer-layer consists in a graphene layer covalently bound to the SiC(0001) substrate through silicon atoms which are arranged in a configuration similar to the deuterated  $(\sqrt{3}\times\sqrt{3})R30^\circ$  reconstruction. We hope that this result will stimulate further experimental and theoretical work in order to assess the proposed bonding environment of the buffer-layer onto the SiC(0001) substrate.

## 5. Summary and perspective

The present vibrational spectroscopic study of the hydrogen (deuterium) adsorption/desorption on the main SiC(0001) reconstructions leading to quasi-free-standing graphene have led to a better understanding of the structural properties of these surfaces. In particular, for the intercalation layer below quasi-free-standing graphene, we gathered indirect evidence that the silicon atoms at the carbon honeycomb interface have a similar environment than the surface silicon atoms of the deuterated  $(\sqrt{3}\times\sqrt{3})R30^\circ$  reconstruction. Another important result of this study concerns the rationalization of the differences in desorption temperature and vibrational frequencies of hydrogen atoms bound to the carbon atoms of the buffer-layer and of the quasi-free-standing graphene (QFMLG). These differences are the result of a different degree of  $sp^2$  hybridization of the carbon atoms at these surfaces, which undergo a partial  $sp^3$  rehybridization on the buffer-layer related to its covalent bonding to the SiC substrate. Additionally, by taking into account the desorption temperature of hydrogen on the silicon atoms of the intercalation layer ( $\sim 1100$  K), we suggest that the intercalation process is possible only in a narrow temperature window (800 – 1050 K) [10] because of the competition with hydrogen adsorption onto the buffer-layer at lower temperature and with hydrogen desorption from the intercalation layer at higher temperature. Finally, since hydrogen desorbs from quasi-free-standing graphene at 600 K we show that the synthesis of hydrogenated QFMLG with hydrogen atoms flux requires a two steps procedure. We hope that these results will encourage further theoretical studies regarding the intercalation process which transforms the  $(6\sqrt{3}\times6\sqrt{3})R30^\circ$  buffer-layer into the QFMLG on SiC(0001) as well as regarding the details of adsorption and desorption properties of hydrogen on these technologically relevant surfaces.

## References

- [1] Geim A K 2009 Graphene: Status and Prospects *Science* **324** 1530–4
- [2] Emtsev K V, Bostwick A, Horn K, Jobst J, Kellogg G L, Ley L, McChesney J L, Ohta T, Reshanov S A, Röhrl J, Rotenberg E, Schmid A K, Waldmann D, Weber H B and Seyller T 2009 Towards wafer-size graphene layers by atmospheric pressure graphitization of silicon carbide *Nat Mater* **8** 203–7
- [3] Ohta T, Bostwick A, McChesney J L, Seyller T, Horn K and Rotenberg E 2007 Interlayer Interaction and Electronic Screening in Multilayer Graphene Investigated with Angle-Resolved Photoemission Spectroscopy *Phys. Rev. Lett.* **98** 206802
- [4] Riedl C, Coletti C, Iwasaki T, Zakharov A A and Starke U 2009 Quasi-Free-Standing Epitaxial Graphene on SiC Obtained by Hydrogen Intercalation *Phys. Rev. Lett.* **103** 246804
- [5] Robinson J A, Hollander M, LaBella M, Trumbull K A, Cavalero R and Snyder D W 2011 Epitaxial Graphene Transistors: Enhancing Performance via Hydrogen Intercalation *Nano Lett.* **11** 3875–80
- [6] Hertel S, Waldmann D, Jobst J, Albert A, Albrecht M, Reshanov S, Schöner A, Krieger M and Weber H B 2012 Tailoring the graphene/silicon carbide interface for monolithic wafer-scale electronics *Nat Commun* **3** 957
- [7] Johns J E and Hersam M C 2013 Atomic Covalent Functionalization of Graphene *Acc. Chem. Res.* **46** 77–86
- [8] Balog R, Jorgensen B, Nilsson L, Andersen M, Rienks E, Bianchi M, Fanetti M, Laegsgaard E, Baraldi A, Lizzit S, Slijivancanin Z, Besenbacher F, Hammer B, Pedersen T G, Hofmann P and Hornekaer L 2010 Bandgap opening in graphene induced by patterned hydrogen adsorption *Nat Mater* **9** 315–9
- [9] Haberer D, Vyalikh D V, Taioli S, Dora B, Farjam M, Fink J, Marchenko D, Pichler T, Ziegler K, Simonucci S, Dresselhaus M S, Knupfer M, Büchner B and Grüneis A 2010 Tunable Band Gap in Hydrogenated Quasi-Free-Standing Graphene *Nano Letters* **10** 3360–6
- [10] Bocquet F C, Bisson R, Themlin J-M, Layet J-M and Angot T 2012 Reversible hydrogenation of deuterium-intercalated quasi-free-standing graphene on SiC(0001) *Phys. Rev. B* **85** 201401
- [11] Goler S, Coletti C, Piazza V, Pingue P, Colangelo F, Pellegrini V, Emtsev K V, Forti S, Starke U, Beltram F and Heun S 2013 Revealing the atomic structure of the buffer layer between SiC(0 0 0 1) and epitaxial graphene *Carbon* **51** 249–54
- [12] Riedl C, Coletti C and Starke U 2010 Structural and electronic properties of epitaxial graphene on SiC(0 0 0 1): a review of growth, characterization, transfer doping and hydrogen intercalation *J. Phys. D: Appl. Phys.* **43** 374009
- [13] Seyller T 2004 Passivation of hexagonal SiC surfaces by hydrogen termination *J. Phys.: Condens. Matter* **16** S1755
- [14] Forti S, Emtsev K V, Coletti C, Zakharov A A, Riedl C and Starke U 2011 Large-area homogeneous quasifree standing epitaxial graphene on SiC(0001): Electronic and structural characterization *Phys. Rev. B* **84** 125449
- [15] Dinger A, Lutterloh C and Küppers J 2000 Stationary and non-stationary etching of Si(100) surfaces with gas phase and adsorbed hydrogen *Chemical Physics Letters* **320** 405–10
- [16] Dinger A, Lutterloh C and Küppers J 2001 Interaction of hydrogen atoms with Si(111) surfaces: Adsorption, abstraction, and etching *J. Chem. Phys.* **114** 5338–50
- [17] Starke U, Schardt J, Bernhardt J, Franke M, Reuter K, Wedler H, Heinz K, Furthmüller J, Käckell P and Bechstedt F 1998 Novel Reconstruction Mechanism for Dangling-Bond Minimization: Combined Method Surface Structure Determination of SiC(111)- (3×3) *Phys. Rev. Lett.* **80** 758–61

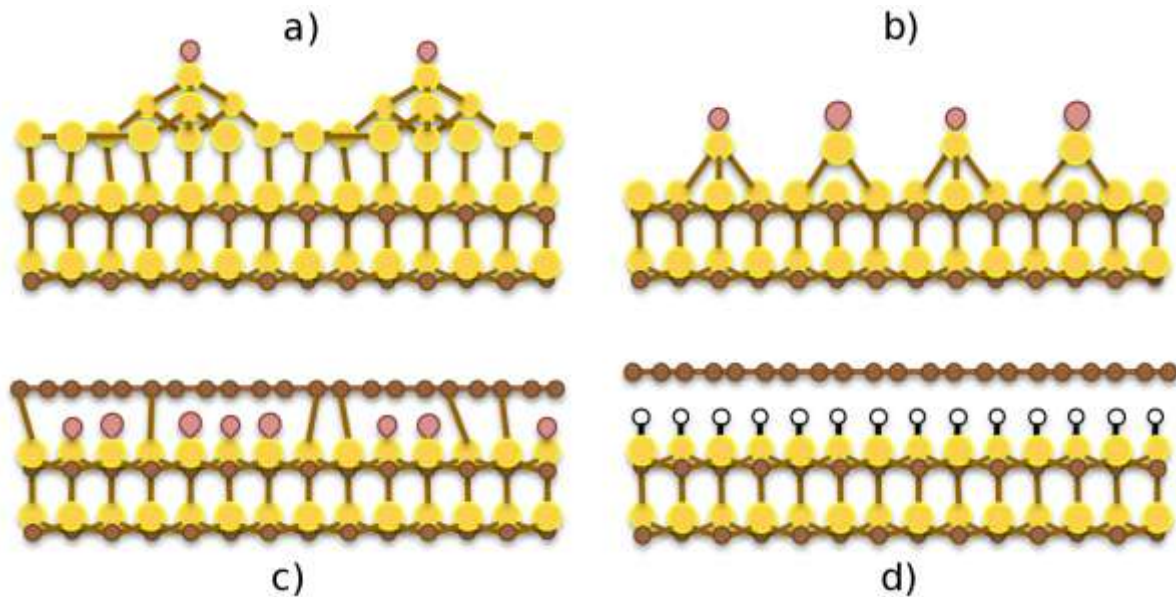
- [18] Schardt J, Bernhardt J, Starke U and Heinz K 2000 Crystallography of the (3×3) surface reconstruction of 3C-SiC(111), 4H-SiC(0001), and 6H-SiC(0001) surfaces retrieved by low-energy electron diffraction *Phys. Rev. B* **62** 10335–44
- [19] Tautz F., Sloboshanin S, Starke U and Schaefer J. 2000 Reassessment of core-level photoemission spectra of reconstructed SiC(0 0 0 1) surfaces *Surface Science* **470** L25–L31
- [20] Stoldt C R, Carraro C and Maboudian R 2000 Deuterium etching of the Si-rich SiC(0001) (3×3) surface reconstruction *Surface Science* **466** 66–72
- [21] Aoki Y and Hirayama H 2009 Hydrogen desorption from 6H-SiC(0001) surfaces during graphitization *Applied Physics Letters* **95** 094103–094103–3
- [22] Van Elsbergen V, Janzen O and Mönch W 1997 Oxidation of clean and H-terminated SiC surfaces *Materials Science and Engineering: B* **46** 366–9
- [23] Takami J, Naitoh M, Yokoh I, Nishigaki S and Toyama N 2001 STM and LEED observation of hydrogen adsorption on the 6H-SiC(0 0 0 1)3×3 surface *Surface Science* **482–485, Part 1** 359–64
- [24] Diani M, Diouri J, Kubler L, Simon L, Aubel D and Bolmont D 2003 6H- AND 4H-SiC(0001) Si SURFACE RICHNESS DOSING BY HYDROGEN ETCHING: A WAY TO REDUCE THE FORMATION TEMPERATURE OF RECONSTRUCTIONS *Surface Review and Letters* **10** 55–63
- [25] Fuchs R and Kliewer K L 1965 Optical Modes of Vibration in an Ionic Crystal Slab *Phys. Rev.* **140** A2076–A2088
- [26] Balster T, Tautz F S, Polyakov V M, Ibach H, Sloboshanin S, Ötting R and Schaefer J A 2006 Strong dispersion of the surface optical phonon of silicon carbide in the near vicinity of the surface Brillouin zone center *Surface Science* **600** 2886–93
- [27] Starke U, Schardt J, Bernhardt J, Franke M and Heinz K 1999 Stacking Transformation from Hexagonal to Cubic SiC Induced by Surface Reconstruction: A Seed for Heterostructure Growth *Phys. Rev. Lett.* **82** 2107–10
- [28] Northrup J E and Neugebauer J 1995 Theory of the adatom-induced reconstruction of the SiC(0001) $\sqrt{3}\times\sqrt{3}$  surface *Phys. Rev. B* **52** R17001–R17004
- [29] Eremtchenko M, Tautz F S, Ötting R and Schaefer J A 2006 Surface phonons of clean, hydrogen- and deuterium-terminated Si(001) surfaces *Surface Science* **600** 3446–55
- [30] Fujino T, Fuse T, Ryu J-T, Inuzuka K, Yamazaki Y, Katayama M and Oura K 2001 Observation of hydrogen adsorption on 6H-SiC(0 0 0 1) surface *Applied Surface Science* **169–170** 113–6
- [31] Tautz F S and Schaefer J A 1998 Ultimate resolution electron energy loss spectroscopy at H/Si(100) surfaces *Journal of Applied Physics* **84** 6636–43
- [32] Forbeaux I, Themlin J-M and Debever J-M 1998 Heteroepitaxial graphite on 6H-SiC(0001): Interface formation through conduction-band electronic structure *Phys. Rev. B* **58** 16396–406
- [33] Qi Y, Rhim S H, Sun G F, Weinert M and Li L 2010 Epitaxial Graphene on SiC(0001): More than Just Honeycombs *Phys. Rev. Lett.* **105** 085502
- [34] Speck F, Jobst J, Fromm F, Ostler M, Waldmann D, Hundhausen M, Weber H B and Seyller T 2011 The quasi-free-standing nature of graphene on H-saturated SiC(0001) *Applied Physics Letters* **99** 122106
- [35] Jayasekera T, Kong B D, Kim K W and Buongiorno Nardelli M 2010 Band Engineering and Magnetic Doping of Epitaxial Graphene on SiC (0001) *Phys. Rev. Lett.* **104** 146801
- [36] Lee B, Han S and Kim Y-S 2010 First-principles study of preferential sites of hydrogen incorporated in epitaxial graphene on 6H-SiC(0001) *Phys. Rev. B* **81** 075432

- [37] Deretzis I and La Magna A 2011 Role of covalent and metallic intercalation on the electronic properties of epitaxial graphene on SiC(0001) *Phys. Rev. B* **84** 235426
- [38] Markevich A, Jones R, Öberg S, Rayson M J, Goss J P and Briddon P R 2012 First-principles study of hydrogen and fluorine intercalation into graphene-SiC(0001) interface *Phys. Rev. B* **86** 045453
- [39] Emtsev K V, Speck F, Seyller T, Ley L and Riley J D 2008 Interaction, growth, and ordering of epitaxial graphene on SiC{0001} surfaces: A comparative photoelectron spectroscopy study *Phys. Rev. B* **77** 155303
- [40] Nie S and Feenstra R M 2009 Tunneling spectroscopy of graphene and related reconstructions on SiC(0001) vol 27 (AVS) pp 1052–7
- [41] Guisinger N P, Rutter G M, Crain J N, First P N and Stroscio J A 2009 Exposure of Epitaxial Graphene on SiC(0001) to Atomic Hydrogen *Nano Letters* **9** 1462–6
- [42] Lambin P, Henrard L, Thiry P, Silien C and Vigneron J P 2003 The dielectric theory of HREELS, a short survey *Journal of Electron Spectroscopy and Related Phenomena* **129** 281–92
- [43] Ng M L, Balog R, Hornekær L, Preobrajenski A B, Vinogradov N A, Mårtensson N and Schulte K 2010 Controlling Hydrogenation of Graphene on Transition Metals *The Journal of Physical Chemistry C* **114** 18559–65
- [44] Guttler A, Zecho T and Küppers J 2004 Adsorption of D(H) atoms on Ar ion bombarded (0001) graphite surfaces *Surf. Sci.* **570** 218–26
- [45] Thomas C, Angot T and Layet J M 2008 Investigation of D(H) abstraction by means of high resolution electron energy loss spectroscopy *Surf. Sci.* **602** 2311–4
- [46] Waclawski B J, Pierce D T, Swanson N and Celotta R J 1982 Direct verification of hydrogen termination of the semiconducting diamond(111) surface *Journal of Vacuum Science and Technology* **21** 368–70
- [47] Aizawa T, Ando T, Kamo M and Sato Y 1993 High-resolution electron-energy-loss spectroscopic study of epitaxially grown diamond (111) and (100) surfaces *Phys. Rev. B* **48** 18348–51
- [48] Thoms B D, Russell J N, Pehrsson P E and Butler J E 1994 Adsorption and abstraction of hydrogen on polycrystalline diamond *The Journal of Chemical Physics* **100** 8425–31
- [49] Thoms B D, Pehrsson P E and Butler J E 1994 A vibrational study of the adsorption and desorption of hydrogen on polycrystalline diamond *Journal of Applied Physics* **75** 1804–10
- [50] Scлаuzero G and Pasquarello A 2012 Carbon rehybridization at the graphene/SiC(0001) interface: Effect on stability and atomic-scale corrugation *Phys. Rev. B* **85** 161405
- [51] De Lima L H, de Siervo A, Landers R, Viana G A, Goncalves A M B, Lacerda R G and Häberle P 2013 Atomic surface structure of graphene and its buffer layer on SiC(0001): A chemical-specific photoelectron diffraction approach *Phys. Rev. B* **87** 081403
- [52] Hornekaer L, Sljivancanin Z, Xu W, Otero R, Rauls E, Stensgaard I, Laegsgaard E, Hammer B and Besenbacher F 2006 Metastable structures and recombination pathways for atomic hydrogen on the graphite (0001) surface *Physical Review Letters* **96** 156104
- [53] Watcharinyanon S, Virojanadara C, Osiecki J R, Zakharov A A, Yakimova R, Uhrberg R I G and Johansson L I 2011 Hydrogen intercalation of graphene grown on 6H-SiC(0001) *Surface Science* **605** 1662–8
- [54] Angot T, Portail M, Forbeaux I and Layet J M 2002 Graphitization of the 6H-SiC(0 0 1) surface studied by HREELS *Surface Science* **502-503** 81–5

- [55] Langer T, Pfnür H, Schumacher H W and Tegenkamp C 2009 Graphitization process of SiC(0001) studied by electron energy loss spectroscopy *Applied Physics Letters* **94** 112106–112106–3
- [56] Lu J, Loh K P, Huang H, Chen W and Wee A T S 2009 Plasmon dispersion on epitaxial graphene studied using high-resolution electron energy-loss spectroscopy *Phys. Rev. B* **80** 113410
- [57] Elias D C, Nair R R, Mohiuddin T M G, Morozov S V, Blake P, Halsall M P, Ferrari A C, Boukhvalov D W, Katsnelson M I, Geim A K and Novoselov K S 2009 Control of Graphene's Properties by Reversible Hydrogenation: Evidence for Graphane *Science* **323** 610–3
- [58] Politano A, Marino A R, Campi D, Farías D, Miranda R and Chiarello G 2012 Elastic properties of a macroscopic graphene sample from phonon dispersion measurements *Carbon* **50** 4903–10
- [59] Politano A, Marino A R and Chiarello G 2012 Phonon dispersion of quasi-freestanding graphene on Pt(111) *Journal of Physics: Condensed Matter* **24** 104025
- [60] Angot T, Bolmont D and Koulmann J J 1996 High resolution electron energy loss spectroscopy study of the Si(001)  $3 \times 1$  hydrogenated surface *Surface Science* **352–354** 401–6

**Table 1:** Summary of hydrogen and deuterium fundamental vibrational frequencies given in meV for adsorption on Si(100) [29,60], SiC(0001) reconstructions measured in this work, graphite [44,45], ion damaged graphite [44,45] and diamond [46–49]. Bending, scissor/umbrella and stretching modes are labeled with  $\delta$ ,  $\chi$  and  $\nu$  respectively. Energy losses peaks related to multiple losses involving the FK phonon are not tabulated. All the additional peaks observed in our measured spectra can be accounted for by adding the fundamental hydrogen (deuterium) frequencies to the fundamental frequency of the FK phonon of typically 115 – 117 meV (e.g. on the buffer-layer surface, the C-D+FK multiple loss appears at 371 meV).

Sample	Mode	Si-D	Si-H	C-D	C-H
Si(100)	$\delta$	51-67	77-81		
	$\chi$	82	112		
	$\nu$	189	259		
(3×3)	$\delta$				
	$\chi$	81			
	$\nu$	189			
$(\sqrt{3}\times\sqrt{3})R30^\circ$	$\delta$	67			
	$\chi$	81			
	$\nu$	192			
Buffer-layer	$\delta$				157
	$\nu$			255	348
QFMLG	$\delta$	67	95		153
	$\nu$	193	263	243	331
Graphite	$\delta$				150
	$\nu$			242	330
Ion-damaged graphite	$\delta$				155
	$\nu$			260	353
Diamond	$\delta$			112	159
	$\nu$			265	363

**Figures:**

**Figure 1:** Ball-and-stick sketches of the SiC(0001) reconstructions studied in this publication: (a)  $(3\times 3)$ , (b)  $(\sqrt{3}\times\sqrt{3})R30^\circ$ , (c)  $(6\sqrt{3}\times 6\sqrt{3})R30^\circ$  buffer-layer, (d) quasi-free-standing monolayer graphene (QFMLG). Silicon, carbon, hydrogen (deuterium) atoms and dangling bonds are represented with yellow spheres, brown spheres, white spheres, and pink blobs, respectively. Size variations of the symbols represent a varying position normal to the figure plane. While precise structural models are still unknown for the buffer-layer and the QFMLG, Starke and coworkers have determined them for the  $(3\times 3)$  [17] and  $(\sqrt{3}\times\sqrt{3})R30^\circ$  [27] reconstructions.

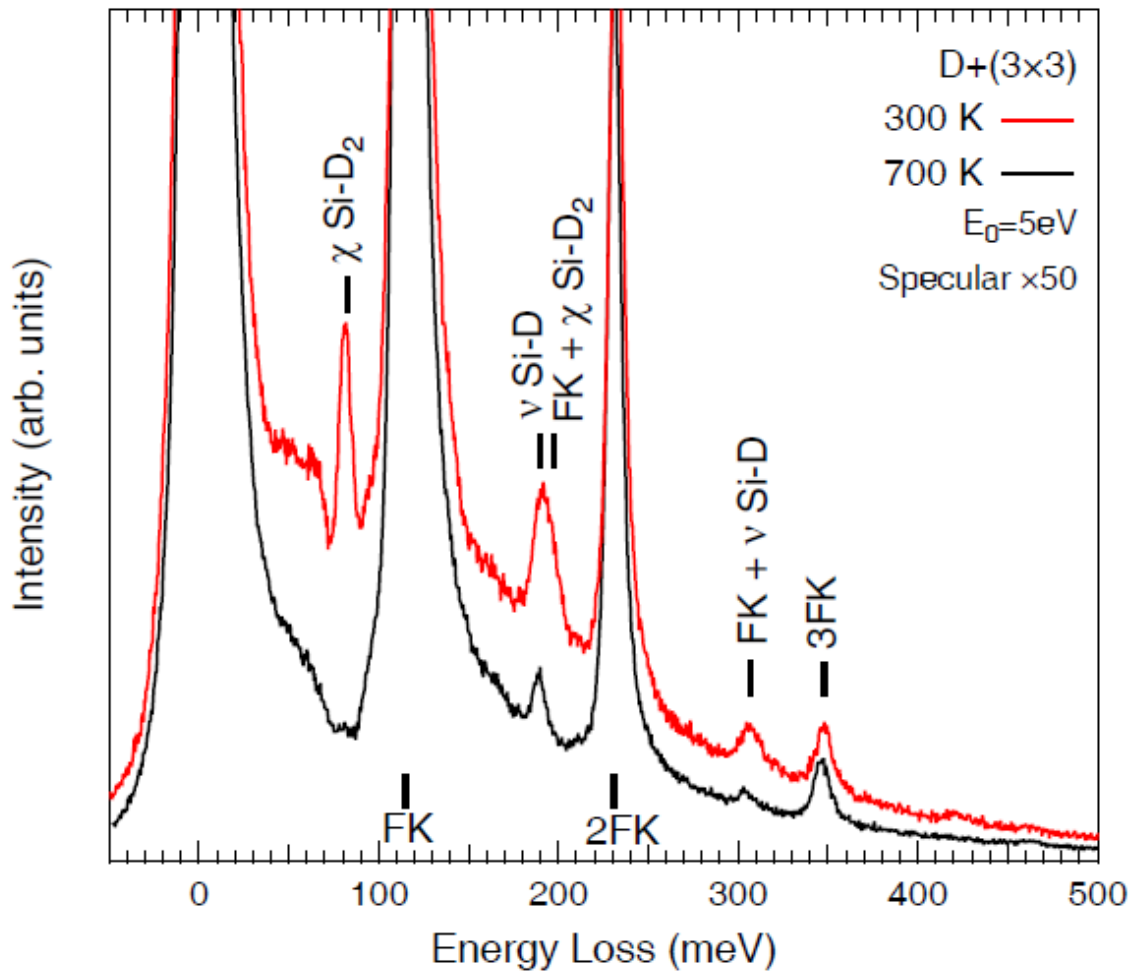


**Figure 2:** HREEL spectra of the (3 $\times$ 3) reconstruction exposed to deuterium atoms at a surface temperature of 700 K (lower black line) and at a surface temperature of 300 K (upper red line). All spectra are taken in the specular direction with an incident energy of 5 eV. Scissor/umbrella and stretching modes are labeled with  $\chi$  and  $\nu$  respectively. SiC Fuchs-Kliwler phonons are identified as 'FK'. Multiple losses are indicated by a linear combination of the aforementioned labels.

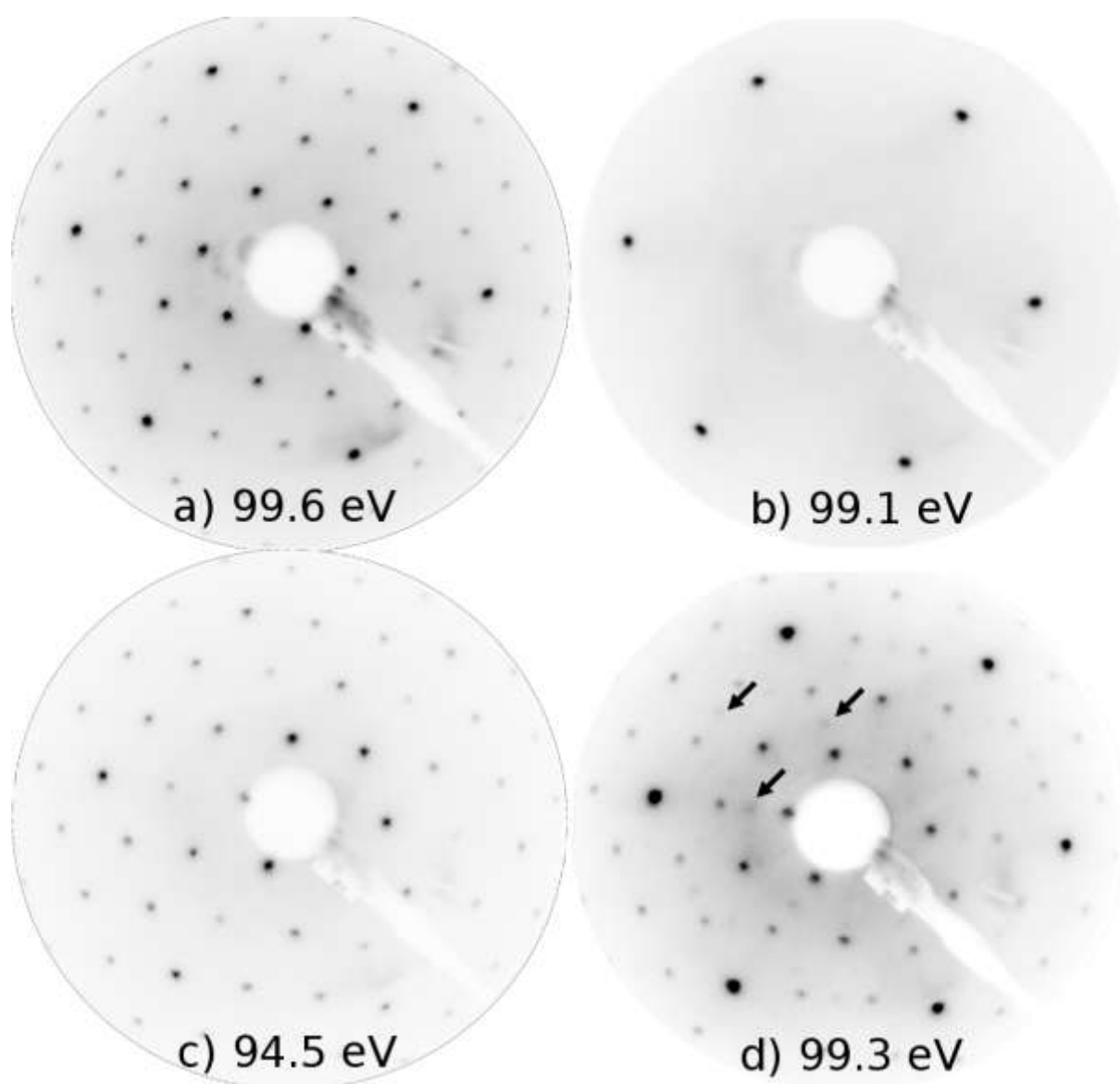


**Figure 3:** LEED patterns of the (3×3) reconstruction: (a) clean, (b) exposed to deuterium at a surface temperature of 700 K, (c) sample in (b) thermally annealed at 850K, (d) exposed to deuterium at a surface temperature of 300 K and thermally annealed at 850 K. Arrows indicate the positions of several extra spots appearing besides the (3×3). The incident beam energy is indicated for each picture.

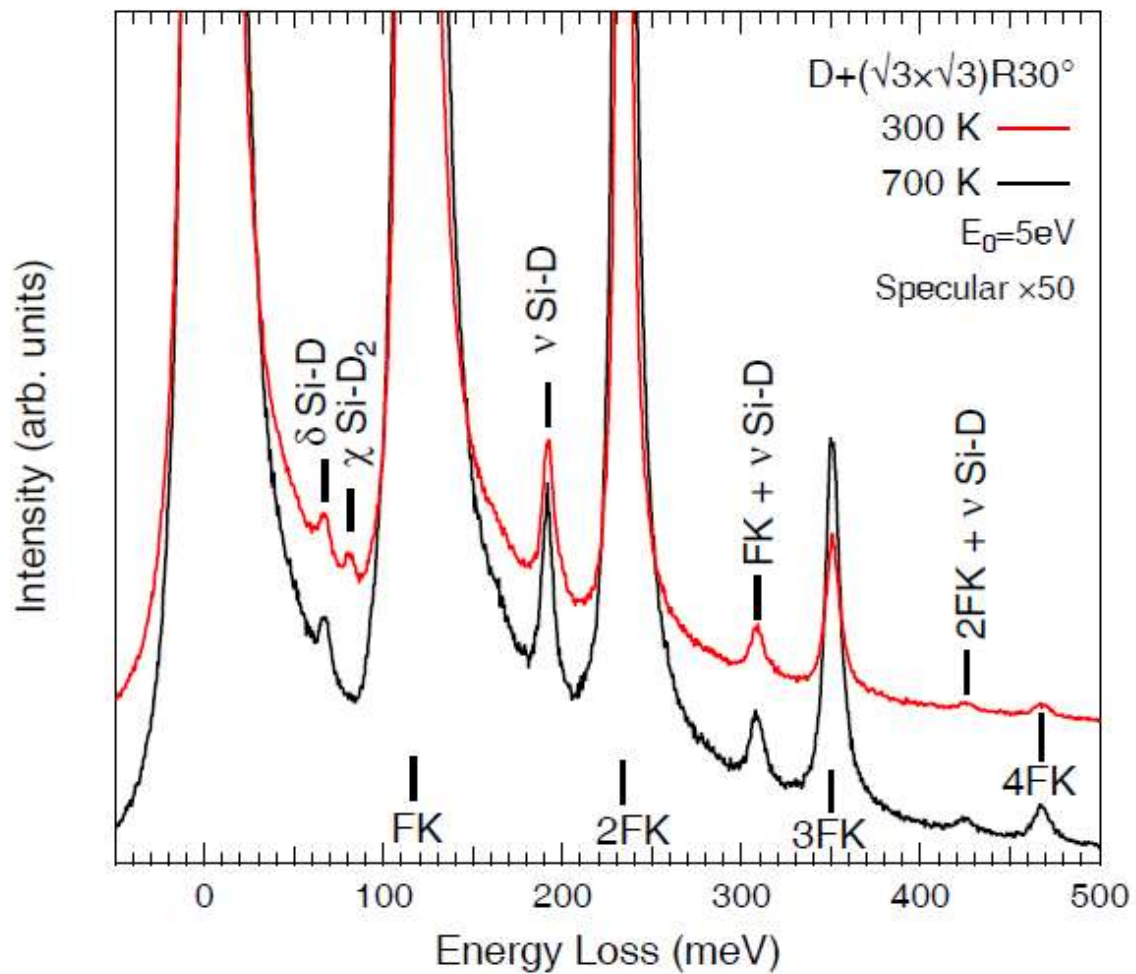


**Figure 4:** HREEL spectra of the  $(\sqrt{3}\times\sqrt{3})R30^\circ$  reconstruction exposed to deuterium atoms at a surface temperature of 700 K (lower black line) and at a surface temperature of 300 K (upper red line). All spectra are taken in the specular direction with an incident energy of 5 eV. Bending, scissor/umbrella and stretching modes are labeled with  $\delta$ ,  $\chi$  and  $\nu$  respectively. SiC Fuchs-Kliwewer phonons are identified as 'FK'. Multiple losses are indicated by a linear combination of the aforementioned labels.

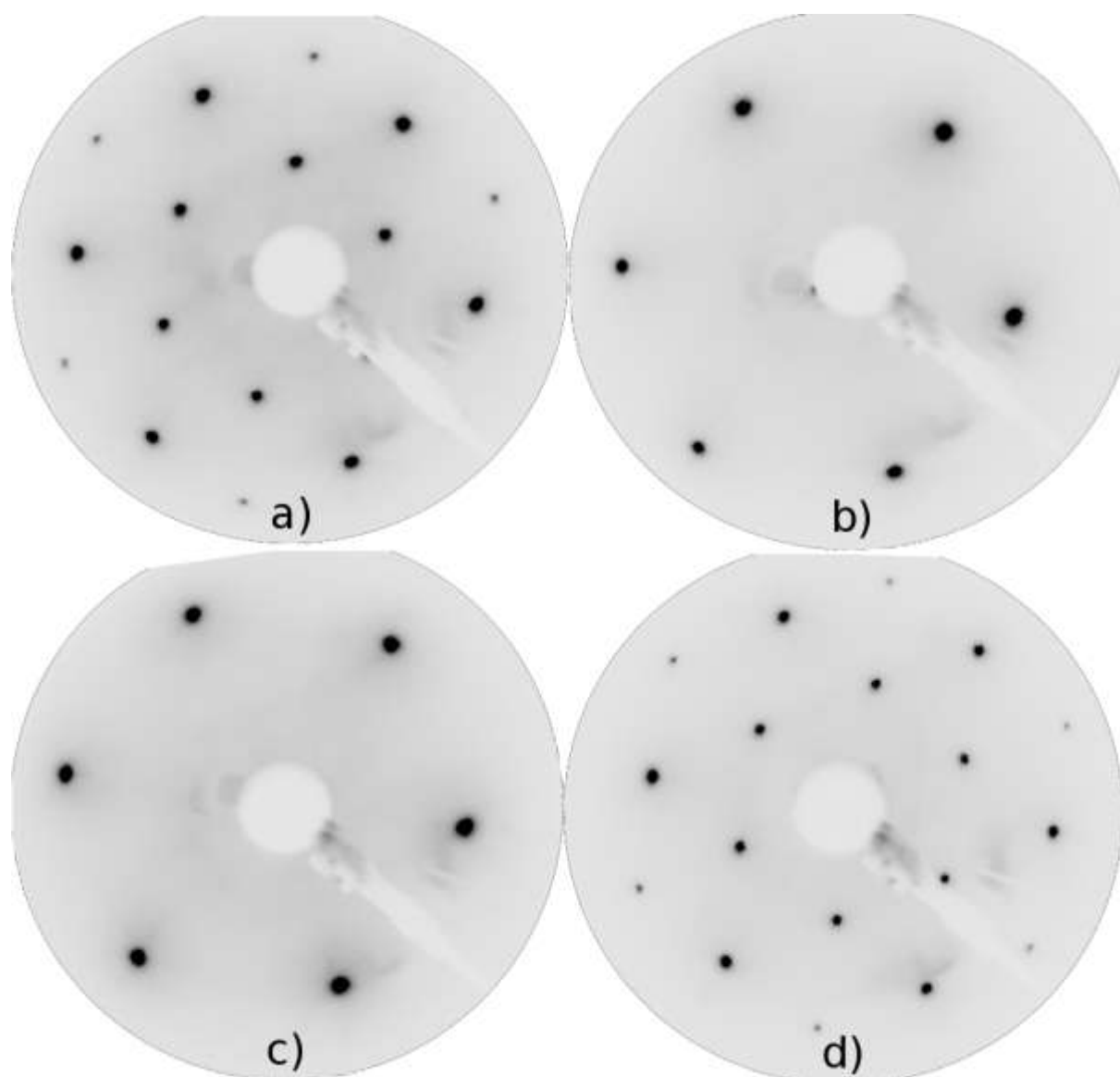


**Figure 5:** LEED patterns of the  $(\sqrt{3}\times\sqrt{3})R30^\circ$  reconstruction: (a) clean, (b) exposed to deuterium at a surface temperature of 700 K, (c) exposed to deuterium at a surface temperature of 300 K, (d) sample in (c) thermally annealed at 1050K. The incident beam energy is 104 eV for all LEED patterns.

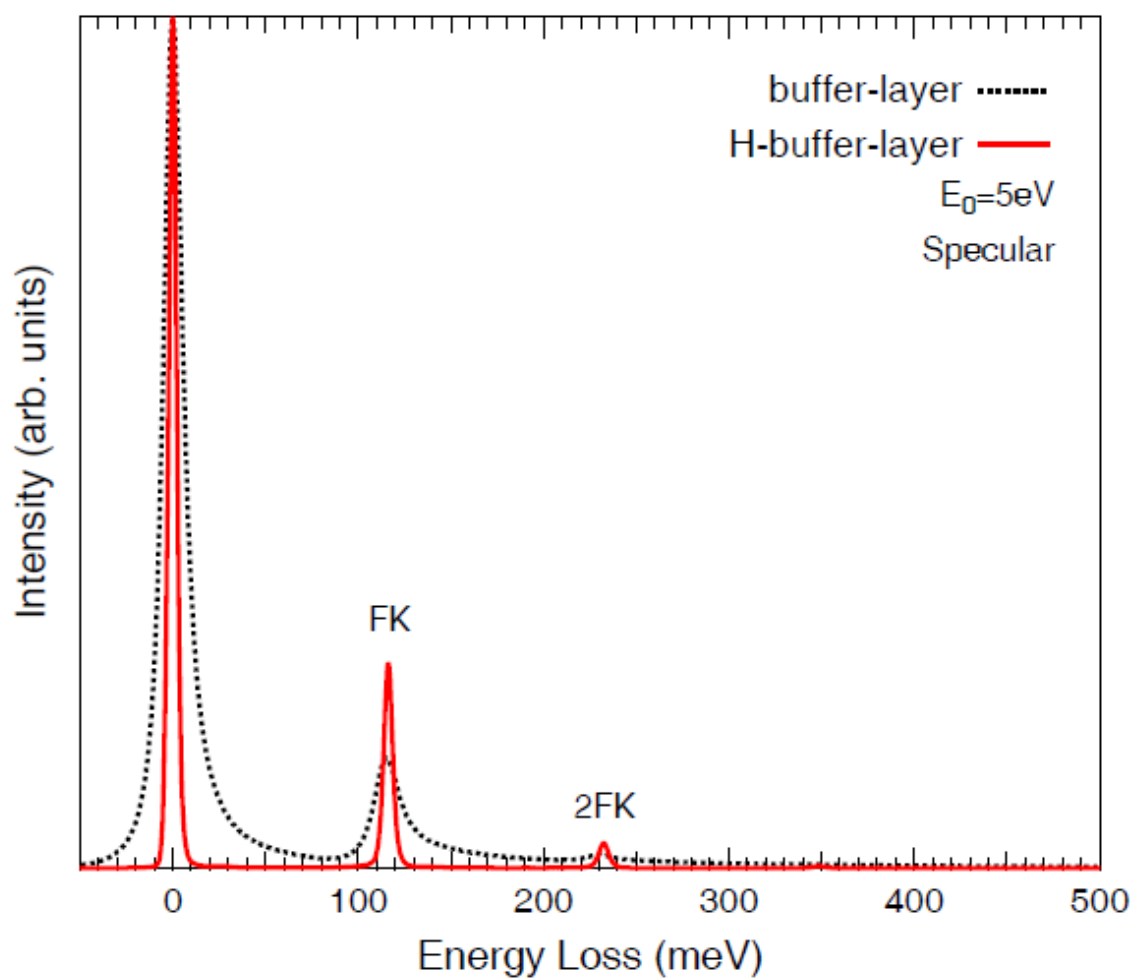


**Figure 6:** HREEL spectra of a clean buffer-layer (black dashed line) and a buffer-layer exposed to hydrogen atoms at a sample temperature of 300 K (red line). All spectra were normalized to the elastic peak maximum and obtained at 5eV incident energy in the specular geometry.

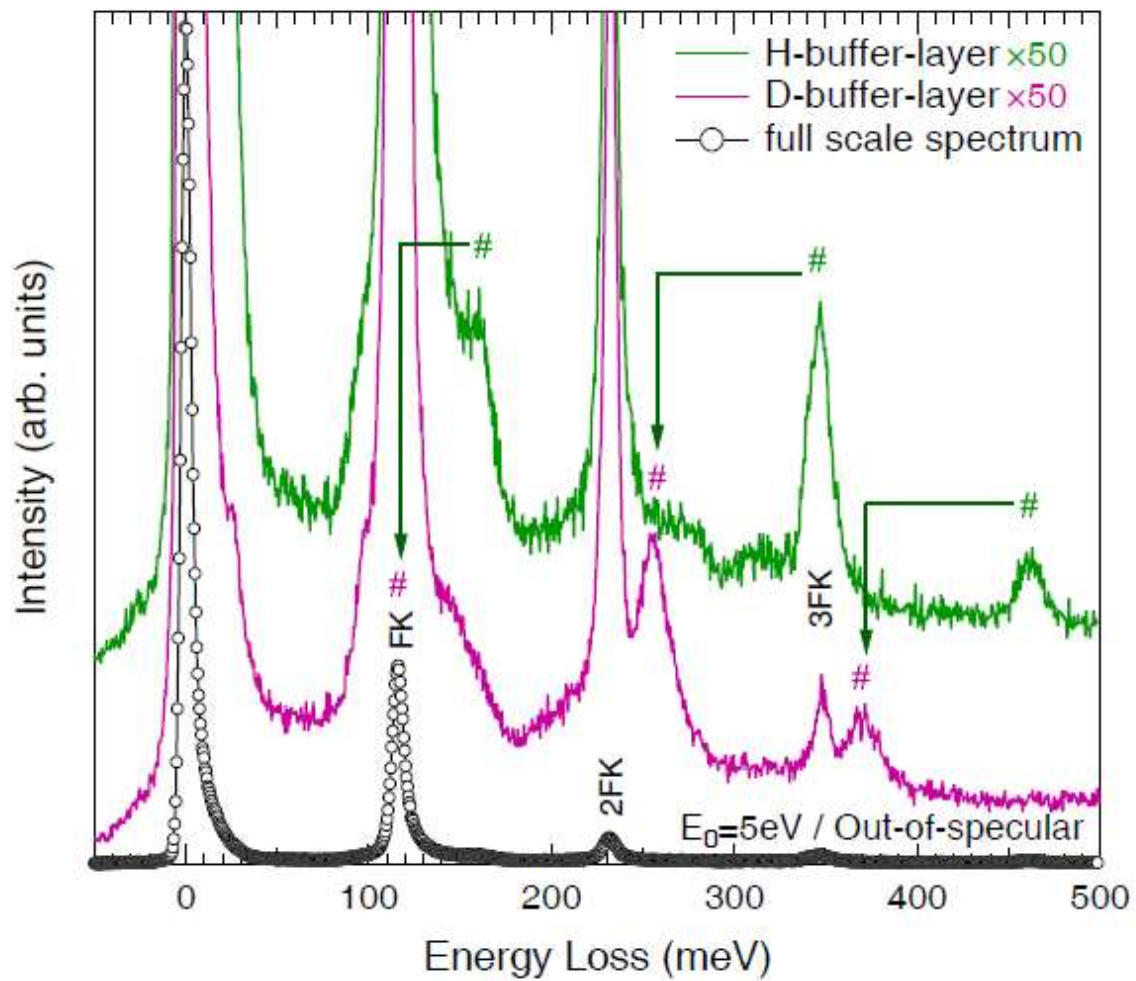


**Figure 7:** HREEL spectra of the hydrogenated buffer-layer (upper green line) and the deuterated buffer-layer (middle magenta line). A full scale spectrum is also shown (lower black circles). The carbon related vibrational modes are marked with sharp symbols. The arrows indicate isotopic shifts from H to D substitution. All spectra were obtained at 5eV incident energy in the out-of-specular geometry.

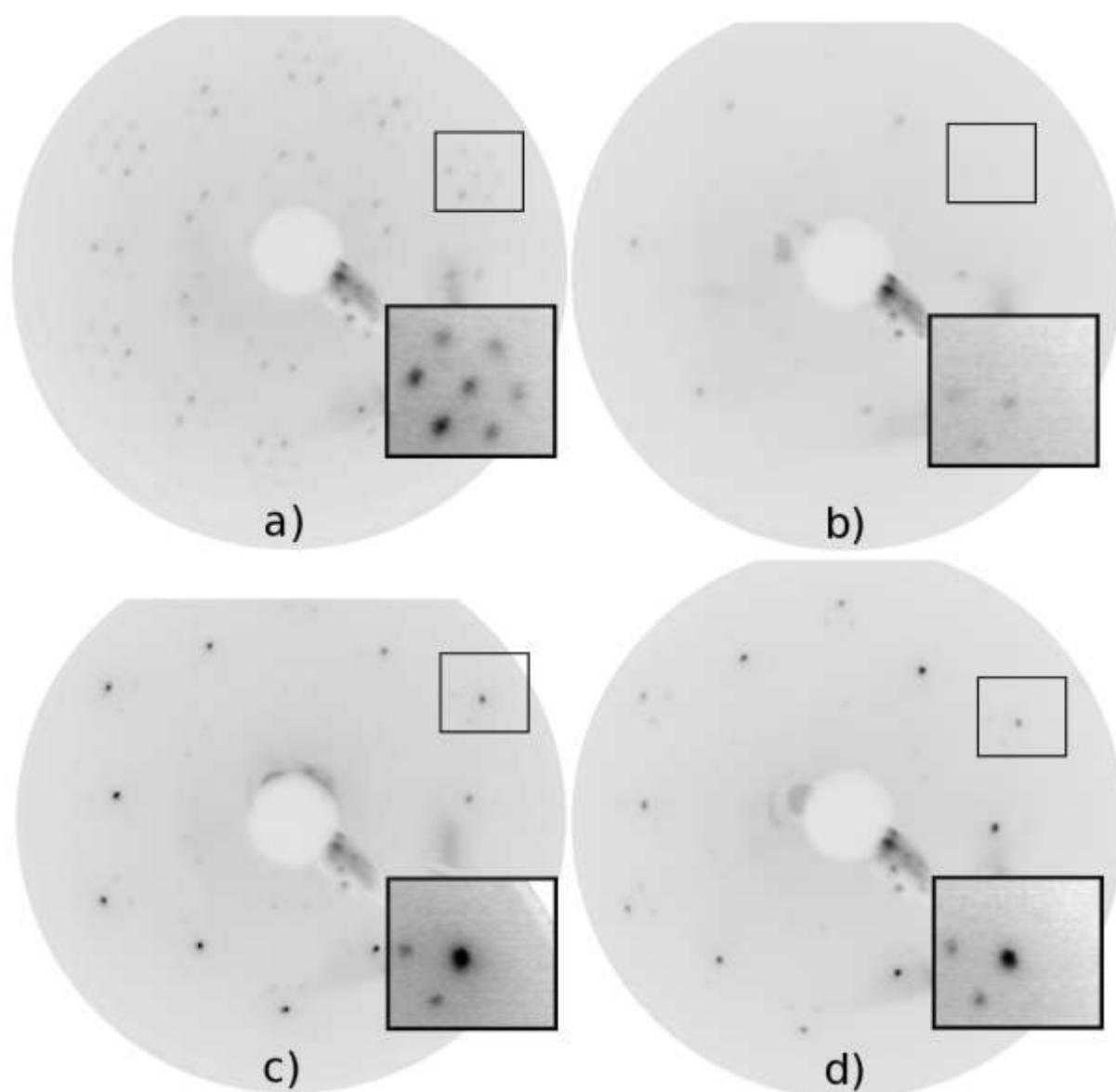


**Figure 8:** LEED patterns of the  $(6\sqrt{3}\times 6\sqrt{3})R30^\circ$  buffer-layer: (a) clean, (b) exposed to hydrogen atoms at a surface temperature of 300 K, and the quasi-free-standing graphene: (c) clean, (d) exposed to hydrogen atoms at a surface temperature of 300 K. The incident beam energy is 140 eV for a) and b) and 126 eV for c) and d). Insets show the buffer-layer (a, b) and the graphene (c, d) regions of the LEED patterns highlighted with black frames. LEED patterns in insets have been processed with identically enhanced contrast.

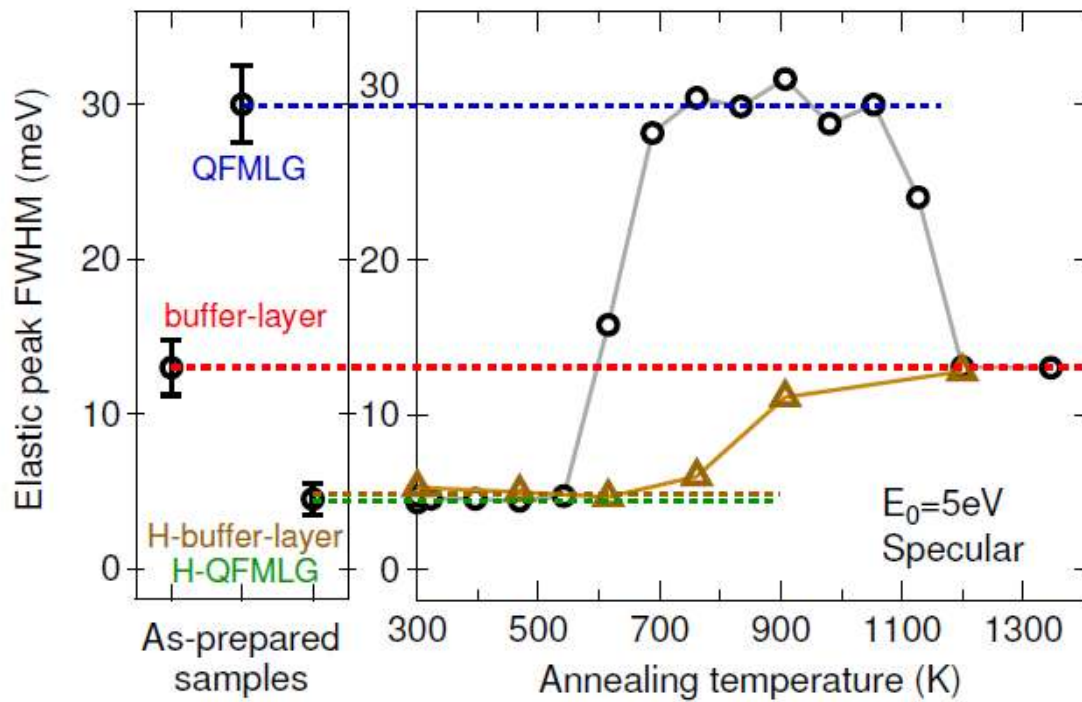


**Figure 9:** HREELS elastic peak FWHM evolution for a hydrogenated QFMLG (black circle) and of a hydrogenated buffer-layer (brown triangle) as a function of the annealing temperature. The horizontal dashed lines indicate the elastic peaks FWHM of aforementioned hydrogenated samples (green and brown), clean QFMLG sample (blue) and clean buffer-layer (red) sample. All measurements were obtained with an incident beam energy of 5eV, in the specular geometry. Figure adapted from [10], copyright 2012 American Physical Society.

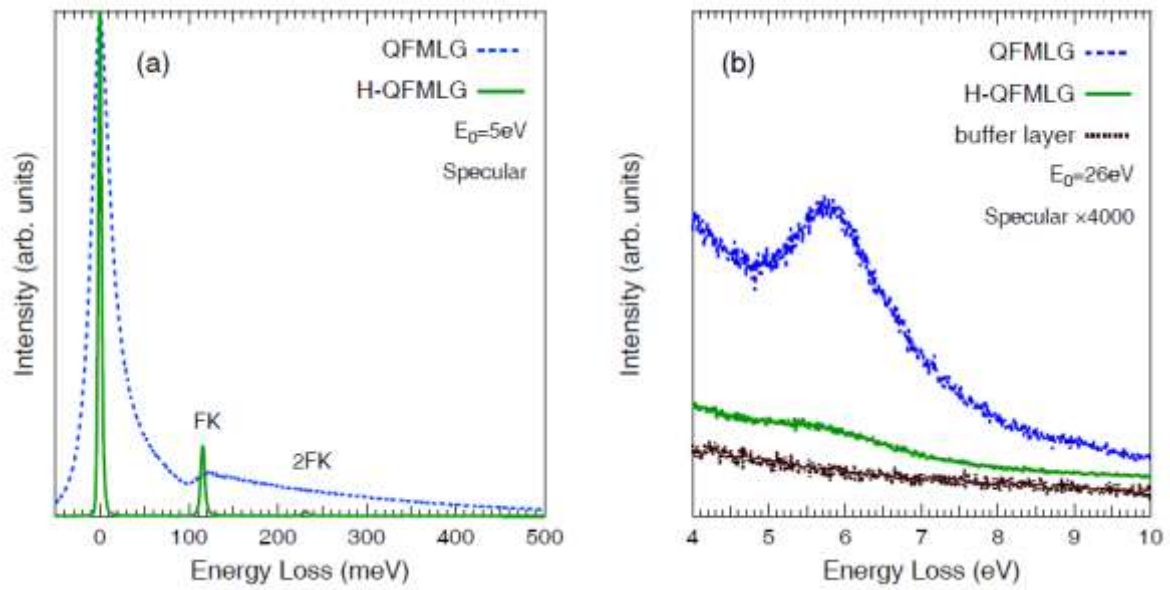


**Figure 10:** HREEL spectra of a quasi-free-standing graphene (upper blue dashed line) and a quasi-free-standing graphene exposed to hydrogen atoms at a sample temperature of 300 K (middle green line) (a) obtained at 5 eV incident energy and (b) obtained at 26 eV incident energy. For the sake of comparison, the buffer-layer spectrum (lower black dotted line) obtained at 26 eV is also depicted in (b). All spectra were normalized to the elastic peak maximum and obtained in the specular geometry.

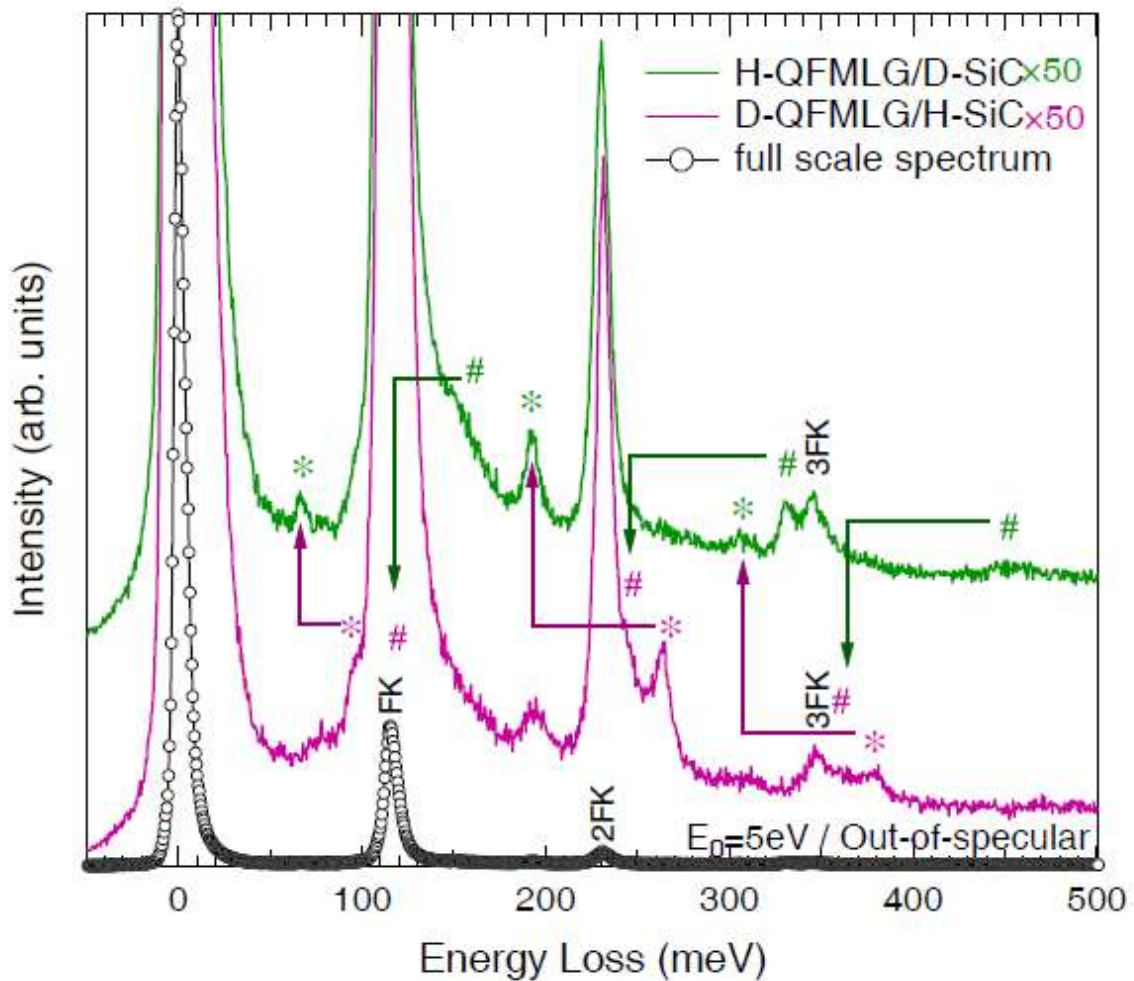


**Figure 11:** HREEL spectra of the QFMLG sample obtained by deuterium intercalation and subsequently hydrogenated (upper green line) and of the QFMLG obtained by hydrogen intercalation and subsequently deuterated (middle magenta line). A full scale spectrum is also shown (lower black circles). The silicon and carbon related vibrational modes are marked with stars and sharp symbols, respectively. The arrows indicate isotopical shifts from H to D substitution. All spectra were obtained at 5eV incident energy in the out-of-specular geometry. Figure adapted from [10], copyright 2012 American Physical Society.